

Published in final edited form as:

Biochemistry. 2011 March 22; 50(11): 1894–1900. doi:10.1021/bi101929e.

An Evolved Aminoacyl-tRNA Synthetase with Atypical Polysubstrate Specificity

Douglas D. Young[†], Travis S. Young[†], Michael Jahnz, Insha Ahmad, Glen Spraggon[§], and Peter G. Schultz^{*}

Department of Chemistry and the Skaggs Institute for Chemical Biology, The Scripps Research Institute, 10550 North Torrey Pines Road, La Jolla, CA 92037, USA

Abstract

We have employed a rapid fluorescence-based screen to assess the polyspecificity of several aaRSs against an array of unnatural amino acids. We discovered that a *p*-cyanophenylalanine specific aminoacyl-tRNA synthetase (*p*CNF-RS) has high substrate permissivity for unnatural amino acids, while maintaining its ability to discriminate against the canonical twenty amino acids. This orthogonal *p*CNF-RS, together with its cognate amber nonsense suppressor tRNA is able to selectively incorporate 18 unnatural amino acids into proteins, including trifluoroketone, alkynyl, and hydrazino substituted amino acids. In an attempt to better understand this polyspecificity, the x-ray crystal structure of the aaRS/*p*-cyanophenylalanine complex was determined. A comparison of this structure with those of other mutant aaRSs showed that both binding site size and other more subtle features control substrate polyspecificity.

Keywords

Unnatural amino acids; *p*-cyanophenylalanine; aminoacyl-tRNA synthetase; polyspecificity

A wide variety of unnatural amino acids (UAAs) have been genetically encoded in bacteria, yeast, and mammalian cells with excellent fidelity and efficiency. These novel amino acids include NMR, IR, fluorescent, and crystallographic probes, orthogonal bioconjugation partners, metal ion chelators, redox active centers, and photocrosslinking and photocaging agents.(1, 2) An orthogonal aminoacyl-tRNA synthetase/suppressor tRNA (aaRS/tRNA_{CUA}) pair (one that does not significantly cross-react with host tRNAs or aminoacyl-tRNA synthetases) is used to selectively incorporate the unnatural amino acid of interest in response to a nonsense or frameshift codon. In order to evolve aaRSs that recognize an unnatural amino acid and no endogenous amino acid, a double sieve selection scheme is employed which ties the activity of the aaRS to the viability of *E. coli*.(3, 4) In the positive selection, large libraries of aaRS active site mutants are screened for their ability to incorporate the unnatural amino acid in response to an amber nonsense codon at a permissive site in an essential protein; in the negative selection, aaRSs that incorporate endogenous amino acids in to a lethal protein in the absence of the unnatural amino acid are removed.

^{*}To whom correspondences should be addressed: Phone: (858) 784-9273, Fax: (858) 784-9440, schultz@scripps.edu.

[†]Authors contributed equally to the work

[§]Genomics Institute of the Novartis Research Foundation

Supporting Information Available: Unnatural amino acids screened and 96-well plate format, myoglobin mass spectral data, and crystal refinement statistics. This material is available free of charge via the Internet at <http://pubs.acs.org>.

Because no selective pressure is applied against other unnatural amino acids during the selection, evolved aaRSs may also cross-react with other unnatural amino acids, while maintaining their orthogonality to endogenous amino acids.(5–9) This polyspecificity can be exploited to incorporate additional unnatural amino acids without the evolution of new, orthogonal aaRS/tRNA pairs. Aminoacyl-tRNA synthetase promiscuity is not problematic in this regard as the growth media can be supplemented with only the desired unnatural amino acid. Previous experiments have examined the substrate permissivity of the pyrrolysyl, *p*-benzoylphenylalanine- and naphthylalanine-synthetases, and mutations were introduced to broaden their substrate specificity. However, a thorough analysis of multiple aminoacyl-tRNA synthetases with a broad range of unnatural amino acid substrates has yet to be realized.^{3a} Thus, to systematically analyze and better understand the permissivity of multiple evolved aaRSs, we have investigated their ability to incorporate a diverse library of unnatural amino acids using a simple fluorescent reporter-based assay.

Experimental Procedures

GFP Expression

GFP expression was carried out as previously described. BL-21 (DE3) *E. coli* was co-transformed with the appropriate pEVOL plasmid and pET-GFP_{Y151X} plasmid(1), grown in 2xYT media at 37 °C to saturation with chloramphenicol (40 µg/mL) and ampicillin (100 µg/mL) and diluted in 2YT to an OD₆₀₀ of 0.2. Diluted cultures were grown at 37 °C to an OD₆₀₀ of 0.7 – 1.0, and induced with IPTG (1 mM) and arabinose (0.02%). The culture was immediately aliquoted (100 µL/well) into a 96 well plate containing 10 µL of 10 mM unnatural amino acid per well and background fluorescence was measured on a Spectramax Gemini EM (Ex/Em= 395/509 nm; Molecular Probes). After 14 h at 30 °C fluorescence was measured again to determine the level of GFP expression. Amino acids that afforded a significantly measurable signal were then employed in similar expression experiments in triplicate. Each sample was normalized to cell density using the OD₆₀₀ and fluorescence was measured and compared to wild type expression (Table 2), confirming the UAA incorporation.

Myoglobin Expression

BL-21(DE3) *E. coli* was co-transformed with the appropriate pEVOL plasmid and pET-Myo_{F107X}, grown in 2xYT media at 37 °C to saturation with chloramphenicol (40 µg/mL) and ampicillin (100 µg/mL) and diluted in 2YT to an OD₆₀₀ of 0.2. Diluted cultures were grown at 37 °C to an OD₆₀₀ of 0.7, induced with IPTG (1 mM), arabinose (0.2%) and the appropriate unnatural amino acid (1 mM) and grown at 37 °C for 16 h. The cultures were pelleted and lysed using Bug Buster (Novagen) and the protein was purified on Ni-NTA spin columns (Qiagen) according to the manufacturer's protocol. Myoglobin expression was analyzed on a 4–20% Gly-Tris polyacrylamide gel (see Supporting Information) and the mass of purified protein was determined by LC/MS on an Agilent 1100 Series LC/MSD. The chromatographic peak corresponding to myoglobin (between 6.1 min and 6.5 min) was charge deconvoluted using Agilent LC/MSD ChemStation software (Rev. B.03.02). Deconvolution parameters were set to high M_r = 17,000 and low M_r = 21,000, maximum charge= 50, and minimum peaks in set = 3 –8. Error± 0.02%, as determined from control samples. Liquid chromatography mass spectrometry results for Myo_{Y107X} expression experiments are listed in the Supporting Information.

Aminoacyl-tRNA synthetase Crystallization

Protein expression and crystallization was carried out as previously described(10–12). The pCNF-RS DNA was amplified from the pBK-CN vector(13) (Fwd Primer: 5' GCAAGCGCATATGGACGAATTTGAAATGA 3'; Rev Primer: 5'

GTTCGGCTCGAGTAATCTCTTTCTAATTG 3'), inserted into the pET-22b(+) vector using the XhoI and NdeI restriction sites, and transformed into BL21(DE3) cells. A 1L 2X YT (Amp) expression culture was inoculated to OD₆₀₀ 0.2 and grown at 37 °C to an OD₆₀₀ of 0.6 and induced with IPTG (1 mM). The culture was grown at 37 °C for 16 h, pelleted and lysed (50 mM NaH₂PO₄, 300 mM NaCl, 10 mM imidazole, 10 mM BME, pH 8.0) by sonication. The sample was then centrifuged (18,000 rpm; 20 min) and the supernatant was incubated with Ni NTA resin (2 mL; Qiagen) for 1 hour at 4 °C. The resin was then washed (100 mL; 50 mM NaH₂PO₄, 300 mM NaCl, 20 mM imidazole, 10 mM BME, pH 8.0) and eluted (5 mL; 50 mM NaH₂PO₄, 300 mM NaCl, 250 mM imidazole, 10 mM BME, pH 8.0), followed by dialysis (3 × 1h rt; 25 mM Tris, 50 mM NaCl, 1 mM EDTA, 10 mM BME, pH 8.0). The aaRS was purified by FPLC on a MonoQ column (Buffer A: 25 mM Tris, 25 mM NaCl, 1 mM EDTA, 10 mM BME, pH 8.5; Buffer B: 25 mM Tris, 1 M NaCl, 1 mM EDTA, 10 mM BME, pH 8.5), concentrated to 2 mL and dialyzed into crystallization buffer (20 mM Tris, 50 mM NaCl, 10 mM BME, pH 8.0). Crystals were grown by the sitting-drop-vapor-diffusion method using a 1:1 mixture of concentrated protein (15 mg/mL, with 2 mM pCNF) and mother liquor (0.2M (NH₄) Tartrate, 20% PEG-3350, pH 6.6) at 20 °C.

Data Collection, Structure Determination and Refinement

Data for the pCNF co-crystals were collected at beamline 5.0.3 of the Advanced Light source (ALS) at a wavelength of 0.9778Å to a maximum Bragg spacing of 2.3Å (Table 1). All data were reduced and scaled using the HKL2000 package(14). The crystal belonged to the monoclinic crystal system with the β angle approaching 90°. A strong peak in the native Patterson map indicated the presence of pseudo-translational symmetry and that the crystal was pseudo-orthorhombic. This was confirmed by the inability of the unreduced data to scale reasonably in the equivalent orthorhombic spacegroup. The presence of non-crystallographic translational symmetry induces considerable deviation from Wilson Statistics. The Wilson Ratio ($\langle I^2 \rangle / \langle I \rangle^2$) for the data set calculated from phenix xtriage is 2.752 and 2.776 for acentric and centric reflections respectively, whereas perfect data should have values of 2.0 and 3.0 respectively. The Wilson distribution, which is based on the assumption of a random distribution of atoms in the cell, is therefore considerably skewed by this translational symmetry and statistics such as the R-factor and procedures such as the calculation of normalized amplitudes which are based on this assumption can be affected. Despite this the structure was easily solved using Phaser(15) using all data between 50 and 2.3Å resolution using the wild type Tyrosyl tRNA synthetase(16) (PDB code 1J1U) as a probe. The molecular replacement solution confirmed the presence of the pseudo-translational symmetry between the two molecules in the asymmetric unit. Electron density produced from an initial refinement with Buster clearly showed the mutated residues between the probe model and the structure as well as electron density for pCNF in both molecules, confirming the validity of the molecular replacement solution. Model building and refinement were performed by iterative building and refinement with Coot and Buster. (17, 18) All other crystallographic manipulations were carried out with the CCP4 program suite.(19) Convergence of the refinement was checked throughout, with weights between geometric and X-ray terms optimized on the basis of the R-free in combination with a criterion for reasonable geometry. The Local Structure Symmetry Restraints (LSSR) procedure was also applied throughout refinement(20), also incorporated based on its effect on the R-free. Validity of the final structure was checked using a combination of the validation tools in Coot (17), including inspection of the Ramachandran plot, real space correlation, rotamer and geometry analysis. Using these refinement and geometrical criteria final model converged with R_{cryst} and R_{free} of 23.0 % and 30.0 % respectively, with excellent geometry, root mean squared deviation (rmsd) of bonds and angles 0.013Å² and 1.3° respectively, no residues in disallowed regions of the Ramachandran plot (Table 1) and all of the mutations in the structure in a preferred rotamer conformation

Results and Discussion

Assay Development

To develop a rapid assay to analyze the incorporation of unnatural amino acids by an evolved aaRS, a fluorescence-based GFP reporter was used. A GFP gene with an amber mutation at Tyr151 (GFP_{Y151X}) was placed under the control of the T7 promoter in a pET101 vector as previously described.(21) Tyrosine 151 is a surface residue that can be substituted with a range of structurally diverse amino acids without affecting protein stability or fluorescence.(21) This reporter affords fluorescence only when the TAG codon is used as a sense codon for the acylated suppressor tRNA_{CUA} (and not a stop codon). Mutant *Methanocaldococcus jannaschii* tyrosyl-RS/tRNA_{CUA} (*Mj*TyrRS/tRNA_{CUA}) pairs encoded in the efficient pEVOL system(21) were co-transformed into BL-21(DE3) cells with the pET-GFP_{Y151X} construct to enable rapid screening for substrate permissivity. Aminoacyl-tRNA synthetases specific for *pAcF* (*p*-acetylphenylalanine, **7**),(22) *pAzF* (*p*-azidophenylalanine, **8**),(23) *pCNF* (*p*-cyanophenylalanine, **1**),(13) *pIF* (*p*-iodophenylalanine, **2**), (24) *pBoF* (*p*-borophenylalanine),(25) *pPrF* (*p*-propargylphenylalanine, **14**),(26) *pCMF* (*p*-carboxymethyl-phenylalanine),(27) *pBpF* (*p*-benzoylphenylalanine),(28) NapA (naphthylalanine),(29) CouA (7-hydroxycoumarin-4-yl ethylglycine),(30) PLA (*p*-hydroxyL-phenyllactic acid),(31) BipyA (bipyridylalanine),(32) and HQA (8-hydroxyquinolin-3-yl alanine),(33) in addition to the wild type tyrosyl-tRNA synthetase, were analyzed.(1, 34) A 96-well format was used to screen 72 unnatural amino acids including *para* and *meta* substituted phenylalanine analogues, histidine and alanine derivatives, amine, biaryl, and thiol containing amino acids (see Supporting Information). While fluorescent amino acids were included in the plate, other than CouA (well E7), the wavelengths of excitation and emission were nonoverlapping with GFP, and a background subtraction prior to expression was sufficient to allow for assessment of incorporation. The fluorescence of each well supplemented with 1 mM amino acid was measured after 14 hours of expression in rich media (Figure 1). In order to rapidly assess amino acid incorporation fluorescence readings were taken on the cultures, as opposed to lysed cells, and potential hits were later confirmed by protein isolation and mass spectrometry.

Many of the aaRSs failed to exhibit a significant degree of substrate promiscuity with respect to the UAA in our screen. Not surprisingly, the wild type *Mj*TyrRS showed no detectable incorporation of any unnatural amino acid in the screen. Additionally, the *pBoF*, *pPrF*, *pCMF*, HQA, CouA, PLA, NapA, and BipyA specific aaRSs displayed a very low propensity for incorporation of unnatural amino acids beyond the specific unnatural amino acid for which they were evolved. The *pAcF*, *pIF* and *pAzF* synthetases were able to incorporate several *para*-substituted phenylalanine analogs included in the screen, but only to a limited extent (see Supporting Information). Most interestingly, *pCNF*-RS(13) exhibited a substantial degree of polyspecificity as it afforded increased GFP_{Y151X} fluorescence in the presence of *p*-chlorophenylalanine (**2**), *p*-fluorophenylalanine (**5**), *p*-acetylphenylalanine (**7**), *p*-alkynylphenylalanine (**6**), benzylserine (**15**), and *p*-phenyl phenylalanine (**12**) (Figure 1). Screen hits were validated by incorporation of the unnatural amino acid into a his-tagged myoglobin mutant containing an F107TAG amber mutation (Myo_{F107X}).(21) The protein was purified using a Ni-NTA resin and analyzed by SDS-PAGE. The calculated mass of purified mutant protein was confirmed by liquid chromatography mass spectroscopy (LCMS). In the absence of any unnatural amino acid low levels of phenylalanine incorporation in response to the amber codon could be detected (< 20%); however, in the presence of any of these amino acids (>1mM), only incorporation of the unnatural amino acid was observed within the detection limits of LCMS.(21) The behavior of *pCNF*-RS in this assay was unique both with respect to incorporation efficiency and substrate diversity relative to the other 13 aminoacyl-tRNA synthetases.

Determination of Substrate Scope for *p*CNF-RS Polyspecificity

The *p*CNF-RS appears to be highly tolerant of *para*-substituted phenylalanine derivatives. Consequently, the *p*CNF-RS was further screened against additional *para*-substituted aromatic amino acids (Figure 2). The majority of these amino acids (**1–18**) were incorporated into GFP_{Y151X} by the *p*CNF-RS (relative incorporation was assessed in triplicate and normalized to cell density, Table 2); incorporation was further validated by incorporation into Myo_{F107X} with subsequent mass spectral analysis (Table 2). *p*CNF-RS substrates include UAAs that have already been genetically encoded in bacteria, e.g., *p*IF (**2**), *p*BrF (*p*-bromophenylalanine **3**), *p*AcF (**7**), *p*AzF (**8**), *p*PrF (**14**), *p*NO₂F (*p*-nitrophenylalanine **11**), *o*NO₂F (*o*-nitrophenylalanine **13**), *O*-methyl Tyr (**16**), and *O*-allyl Tyr (**17**). *p*CNF-RS substrates also include unnatural amino acids which have not previously been encoded in bacteria, e.g., *p*CIF (**4**), *p*FF (**5**), *p*-ethynyl phenylalanine (**6**), *p*-trifluoromethylacetyl phenylalanine (**9**), *p*-phenyl phenylalanine (**12**), benzylserine (**15**), and *O*-tert-butyl tyrosine (**18**). Based on GFP expression levels, many of the amino acids are good substrates for *p*CNF-RS, affording >80% protein expression relative to wild type GFP. Interestingly, several amino acids (*p*IF (**2**), *p*BrF (**3**), *p*CIF (**4**), *p*-alkynylF (**6**), *p*AzF (**8**), *p*-isopropylF (**10**), and OMeY (**16**)) afford higher protein yields than did the *p*CNF substrate (**1**), the UAA against which the *p*CNF-RS was originally selected. Only amino acids **19–21** (*p*-carboxyphenylalanine, *p*-methyl-phosphonic acid phenylalanine, and *p*-aminophenylalanine), which have hydrogen bond donating substituents, were not incorporated. It is interesting to note that despite the apparent polysubstrate specificity of the *p*CNF-RS, **21** (*p*-aminophenylalanine) was not incorporated while other significantly larger substituents were tolerated, indicating the *p*CNF-RS has some degree of specificity (**21** has been previously shown to be taken up efficiently by *E. coli* and is stable in the cytoplasm). (35) In total, the *p*CNF-RS was found to incorporate 18 unnatural amino acids, seven of which had not been previously encoded. A number of the latter UAAs, e.g., *p*-alkynylphenylalanine (**6**) and *p*-trifluoroacetylphenylalanine (**9**), may be useful as orthogonal bioconjugation handles or as warheads for the selective inactivation of enzymes.

X-ray Crystal Structure of *p*CNF-RS

To better understand the molecular basis of *p*CNF-RS's polysubstrate specificity (which in contrast to polyspecific enzymes like p450s, is not a solvent exposed surface cavity), the aaRS was overexpressed and crystallized for x-ray structure analysis (10–12, 36). The crystal structure of the *p*CNF-RS *p*CNF complex was solved to 2.3 Å with an R_{factor} = 0.23 (Table 1 and Supporting Information). The *p*CNF-RS structure superimposes well onto the WT-TyrRS-Tyr structure (PDB 1J1U) except in the amino acid binding site. The amino acid binding site for the *p*CNF-RS is relatively hydrophobic containing the following mutations relative to the wild type synthetase: Y32L, L65V, F108W, N109M, D158G, and I159A. A comparison of the WT-TyrRS structure to the *p*CNF bound *p*CNF-RS structure (Figure 4A vs. Figure 4B) reveals that mutations create a larger binding pocket which allows the enzyme to accept the nitrile group. In the WT-TyrRS structure, residues Y32 and D158 are involved in hydrogen bonding with the tyrosine hydroxyl group. These residues in the *p*CNF-RS are mutated to leucine and glycine, respectively, which removes hydrogen bonding potential and likely explains the inability of *p*CNF-RS to accept tyrosine and other phenylalanine derivatives with hydrogen bond donor substituents in the *para* position. Additionally, the mutation L65V creates a larger binding pocket and appears to alter the angular position of the bound amino acid. This mutation is unique to the *p*CNF-RS, as no other previously evolved aminoacyl-tRNA synthetases possess the valine residue at this position. Although the binding pocket is larger in *p*CNF-RS, key residues (Leu 32, Val65 and Gly158) are still able to stabilize the *p*CNF (**1**) through van Der Waals interactions (Figure 4B).

To determine which mutations might be determinants of polyspecificity, the *p*CNF bound *p*CNF-RS amino acid binding site structure was overlaid with the substrate-bound *p*AcF-RS (Y32L, D158G, I159C, L162R; PDB 1ZH6) and NapA-RS (Y32L, D158P, I159A, L162Q, A167V; PDB 1ZH0) structures. The former aaRS accepts relatively few other unnatural amino acids, while the latter displays no polyspecificity (Figure 3). As previously noted, the Y32L mutation increases the amino acid binding site size (especially at the *para*-position of phenylalanine derivatives); however, this mutation is also found in the *p*AcF-RS and NapA-RS (among others), which do not exhibit a comparable degree of polyspecificity to *p*CNF-RS. The unique L65V mutation appears to create unoccupied space at the back of the amino acid binding that is filled by other residues in *p*AcF-RS. This mutation may enable *p*CNF-RS to accept a diverse group of *para*-substituted phenylalanine or tyrosine derivatives (Figure 3). Interestingly, when *p*CNF is modeled into the *p*AcF-RS binding pocket, the leucine at residue 65 interferes with the cyano substituent (Figure 4C; the *p*AcF-RS complex is shown for comparison in Figure 4F). In contrast, *p*AcF (**7**) can readily be docked into the active site of the *p*CNF-RS (Figure 4E). Additionally, mutation of leucine 65 to smaller amino acids has been shown to allow the incorporation of larger unnatural amino acids in other aaRSs. For example, the *o*-nitrobenzyl tyrosine (ONBY) synthetase contains a L65G mutation, facilitating the incorporation of the sterically bulky bicyclic ONBY amino acid. (37)

While an increased substrate binding site size may be partially responsible for increased polyspecificity, other factors are involved. This is apparent when comparing the *p*CNF-RS and NapA-RS structures. Although the D158P mutation in the NapA-RS gives it a significantly larger binding pocket than the *p*CNF-RS, this aaRS exhibits virtually no permissivity. When *p*CNF is modeled into the amino acid binding site of NapA-RS, proline 158 prevents side chain Van der Waals interactions that might stabilize the bound amino acid (Figure 4D). Moreover, a number of the other aminoacyl-tRNA synthetases examined with larger binding sites (e.g., that accommodate bipyridyl, 8-hydroxyquinolyl and benzoylphenyl side chains) do not show significant polyspecificity, suggesting that there is a plasticity unique to *p*CNF-RS active site.

The uniqueness of the *p*CNF-RS is also evident when examining backbone perturbations in the mutant aminoacyl-tRNA synthetases. As previously reported, the D158P and I159A mutations terminate the α_8 -helix in NapA-RS; a similar backbone alteration is observed in the *p*AcF-RS (albeit to a lesser extent). (12) Interestingly, this perturbation is not observed in the *p*CNF-RS, despite having the same D158G mutation as the *p*AcF-RS and the same I159A mutation as the NapA-RS. In fact, the *p*CNF-RS aligns much more closely to the wild-type tyrosyl-tRNA synthetase than with the other aminoacyl-tRNA synthetases in this region (Figure 5A). Another distinctive difference is apparent in the *p*CNF-RS when examining the helical residues 108 and 109. Relative to both the WT-RS and the *p*AcF-RS, the helix is moderately displaced and is slightly truncated (Figure 5B). This may afford a greater degree of space and plasticity for the accommodation of larger *para*-substituted amino acids.

Importantly, the *p*CNF-RS amino acid binding site still highly discriminates against Phe, Tyr and *p*-aminophenylalanine, while it accepts similar amino acid such as *O*-methyltyrosine (**16**), *p*-chlorophenylalanine (**4**) and *p*-fluorophenylalanine (**5**). Clearly, mutations in a relatively small number of active site residues result in the ability of this aaRS to discriminate subtle changes in substrate structure. This result indicates that the negative selection step in the evolution of *p*CNF-RS is quite robust in its ability to remove polyspecific mutants that accept endogenous amino acids. Work is currently underway to co-crystallize *p*CNF-RS and various mutants with additional common and unnatural amino acids in an effort to further decipher this unique enzyme's specificity.

Conclusion

The use of previously evolved aaRSs for the incorporation of additional unnatural amino acids will facilitate the expansion of the genetic repertoire to include novel chemical functionalities. Seven amino acids which had previously not been genetically encoded in bacteria were selectively incorporated into proteins using the *p*CNF-RS synthetase. These include *p*-chlorophenylalanine, *p*-fluorophenylalanine, *p*-alkynylphenylalanine (**4-6**), *p*-trifluoromethylacetylphenylalanine (**9**), *p*-phenyl phenylalanine (**12**), benzylserine (**15**), and O-*tert*-butyl tyrosine (**18**). Future screens of additional amino acids and aaRSs may yields aaRSs that incorporate classes of unnatural amino acids rather than a single residue.

Supplementary Material

Refer to Web version on PubMed Central for supplementary material.

Acknowledgments

This work was funded by grant DE-FG03-00ER46051 from the Division of Materials Sciences, DOE (P.G.S.). This is manuscript 20691 of the Scripps Research Institute.

D.D.Y. is grateful for a NIH fellowship IF32CA144213 and T.S.Y. is grateful for an Achievement Rewards for College Scientists Scholarship. The work in this paper is based on experiments conducted at beamline 5.0.3 of the advanced light source (ALS). The ALS is supported by the Director, Office of Science, Office of Basic Energy Sciences, Material Sciences Division of the U.S. Department of Energy under contract No. DE-AC03-76SF00098 at Lawrence Berkeley National Laboratory. We would like to thank all of the staff of these beamlines for their continued support.

References

1. Young TS, Schultz PG. Beyond the Canonical 20 Amino Acids: Expanding the Genetic Lexicon. *J Biol Chem*. 2010
2. Liu CC, Schultz PG. An Expanding Genetic Code. *Annual Review of Biochemistry*. 2010;79.
3. Wang L, Schultz PG. A general approach for the generation of orthogonal tRNAs. *Chem Biol*. 2001; 8:883–890. [PubMed: 11564556]
4. Santoro SW, Wang L, Herberich B, King DS, Schultz PG. An efficient system for the evolution of aminoacyl-tRNA synthetase specificity. *Nat Biotechnol*. 2002; 20:1044–1048. [PubMed: 12244330]
5. Stokes AL, Miyake-Stoner SJ, Peeler JC, Nguyen DP, Hammer RP, Mehl RA. Enhancing the utility of unnatural amino acid synthetases by manipulating broad substrate specificity. *Mol Biosyst*. 2009; 5:1032–1038. [PubMed: 19668869]
6. Hartman MC, Josephson K, Lin CW, Szostak JW. An expanded set of amino acid analogs for the ribosomal translation of unnatural peptides. *PLoS One*. 2007; 2:e972. [PubMed: 17912351]
7. Miyake-Stoner SJ, Refakis CA, Hammill JT, Lusich H, Hazen JL, Deiters A, Mehl RA. Generating permissive site-specific unnatural aminoacyl-tRNA synthetases. *Biochemistry*. 2010; 49:1667–1677. [PubMed: 20082521]
8. Kirshenbaum K, Carrico IS, Tirrell DA. Biosynthesis of proteins incorporating a versatile set of phenylalanine analogues. *Chembiochem*. 2002; 3:235–237. [PubMed: 11921403]
9. Munier R, Cohen GN. Incorporation of structural analogues of amino acids into bacterial proteins during their synthesis in vivo. *Biochim Biophys Acta*. 1959; 31:378–391. [PubMed: 13628664]
10. Liu W, Alfonta L, Mack AV, Schultz PG. Structural basis for the recognition of para-benzoyl-L-phenylalanine by evolved aminoacyl-tRNA synthetases. *Angew Chem Int Ed Eng*. 2007; 146:6073–6075.
11. Turner JM, Graziano J, Spraggon G, Schultz PG. Structural characterization of a *p*-acetylphenylalanyl aminoacyl-tRNA synthetase. *J Am Chem Soc*. 2005; 127:14976–14977. [PubMed: 16248607]

12. Turner JM, Graziano J, Spraggon G, Schultz PG. Structural plasticity of an aminoacyl-tRNA synthetase active site. *Proc Natl Acad Sci U S A*. 2006; 103:6483–6488. [PubMed: 16618920]
13. Schultz KC, Supekova L, Ryu Y, Xie J, Perera R, Schultz PG. A genetically encoded infrared probe. *J Am Chem Soc*. 2006; 128:13984–13985. [PubMed: 17061854]
14. Otwinowski Z, Minor W. Processing of X-ray diffraction data collected in oscillation mode. *Method Enzymo*. 1997; 1276:307–326.
15. McCoy AJ, Grosse-Kunstleve RW, Storoni LC, Read RJ. Likelihood-enhanced fast translation functions. *Acta Crystallogr D*. 2005; 61:458–464. [PubMed: 15805601]
16. Kobayashi T, Nureki O, Ishitani R, Yaremchuk A, Tukalo M, Cusack S, Sakamoto K, Yokoyama S. Structural basis for orthogonal tRNA specificities of tyrosyl-tRNA synthetases for genetic code expansion. *Nat Struct Biol*. 2003; 10:425–432. [PubMed: 12754495]
17. Emsley P, Cowtan K. Coot: model-building tools for molecular graphics. *Acta Crystallogr D*. 2004; 60:2126–2132. [PubMed: 15572765]
18. Bricogne, G.; Blanc, E.; Brandl, M.; Flensburg, C.; Keller, P.; Paciorek, P.; Roversi, P.; Sharff, A.; Smart, O.; Vornrhein, C.; Womack, T. BUSTER version 2.9. Global Phasing Ltd; Cambridge, United Kingdom: 2010.
19. Bailey S. The Ccp4 Suite - Programs for Protein Crystallography. *Acta Crystallogr D*. 1994; 50:760–763. [PubMed: 15299374]
20. Smart O, Brandl M, Flensburg C, Keller P, Paciorek W, Wornrhein C, Womack T, Bricogne G. Refinement with Local Structure Similarity Restraints (LSSR) Enables Exploitation of Information from Related Structures and Facilitates use of NCS. *Abstr Annu Meet Am Crystallogr Assoc*. 2008:117.
21. Young TS, Ahmad I, Yin JA, Schultz PG. An Enhanced System for Unnatural Amino Acid Mutagenesis in *E. coli*. *J Mol Biol*. 2009; 10.1016/j.jmb.2009.10.030
22. Wang L, Zhang ZW, Brock A, Schultz PG. Addition of the keto functional group to the genetic code of *Escherichia coli*. *P Natl Acad Sci USA*. 2003; 100:56–61.
23. Chin JW, Santoro SW, Martin AB, King DS, Wang L, Schultz PG. Addition of p-azido-L-phenylalanine to the genetic code of *Escherichia coli*. *Journal of the American Chemical Society*. 2002; 124:9026–9027. [PubMed: 12148987]
24. Xie JM, Wang L, Wu N, Brock A, Spraggon G, Schultz PG. The site-specific incorporation of p-iodo-L-phenylalanine into proteins for structure determination. *Nature Biotechnology*. 2004; 22:1297–1301.
25. Brustad E, Bushey ML, Lee JW, Groff D, Liu W, Schultz PG. A Genetically Encoded Boronate-Containing Amino Acid. *Angew Chem Int Edit*. 2008; 47:8220–8223.
26. Deiters A, Schultz PG. In vivo incorporation of an alkyne into proteins in *Escherichia coli*. *Bioorg Med Chem Lett*. 2005; 15:1521–1524. [PubMed: 15713420]
27. Xie JM, Supekova L, Schultz PG. A genetically encoded metabolically stable analogue of phosphotyrosine in *Escherichia coli*. *Acs Chemical Biology*. 2007; 2:474–478. [PubMed: 17622177]
28. Chin JW, Martin AB, King DS, Wang L, Schultz PG. Addition of a photocrosslinking amino acid to the genetic code of *Escherichia coli*. *P Natl Acad Sci USA*. 2002; 99:11020–11024.
29. Wang L, Brock A, Schultz PG. Adding L-3-(2-naphthyl)alanine to the genetic code of *E. coli*. *Journal of the American Chemical Society*. 2002; 124:1836–1837. [PubMed: 11866580]
30. Wang JY, Xie JM, Schultz PG. A genetically encoded fluorescent amino acid. *Journal of the American Chemical Society*. 2006; 128:8738–8739. [PubMed: 16819861]
31. Guo JT, Wang JY, Anderson JC, Schultz PG. Addition of an alpha-hydroxy acid to the genetic code of bacteria. *Angew Chem Int Edit*. 2008; 47:722–725.
32. Xie JM, Liu WS, Schultz PG. A genetically encoded bidentate, metal-binding amino acid. *Angew Chem Int Edit*. 2007; 46:9239–9242.
33. Lee HS, Spraggon G, Schultz PG, Wang F. Genetic Incorporation of a Metal-Ion Chelating Amino Acid into Proteins as a Biophysical Probe. *Journal of the American Chemical Society*. 2009; 131:2481. [PubMed: 19193005]

34. Guo J, Wang J, Lee JS, Schultz PG. Site-specific incorporation of methyl- and acetyl-lysine analogues into recombinant proteins. *Angew Chem Int Ed Eng*. 2008; 147:6399–6401.
35. Mehl RA, Anderson JC, Santoro SW, Wang L, Martin AB, King DS, Horn DM, Schultz PG. Generation of a bacterium with a 21 amino acid genetic code. *Journal of the American Chemical Society*. 2003; 125:935–939. [PubMed: 12537491]
36. Zhang Y, Wang L, Schultz PG, Wilson IA. Crystal structures of apo wild-type *M. jannaschii* tyrosyl-tRNA synthetase (TyrRS) and an engineered TyrRS specific for O-methyl-L-tyrosine. *Protein Sci*. 2005; 14:1340–1349. [PubMed: 15840835]
37. Deiters A, Groff D, Ryu YH, Xie JM, Schultz PG. A genetically encoded photocaged tyrosine. *Angew Chem Int Edit*. 2006; 45:2728–2731.

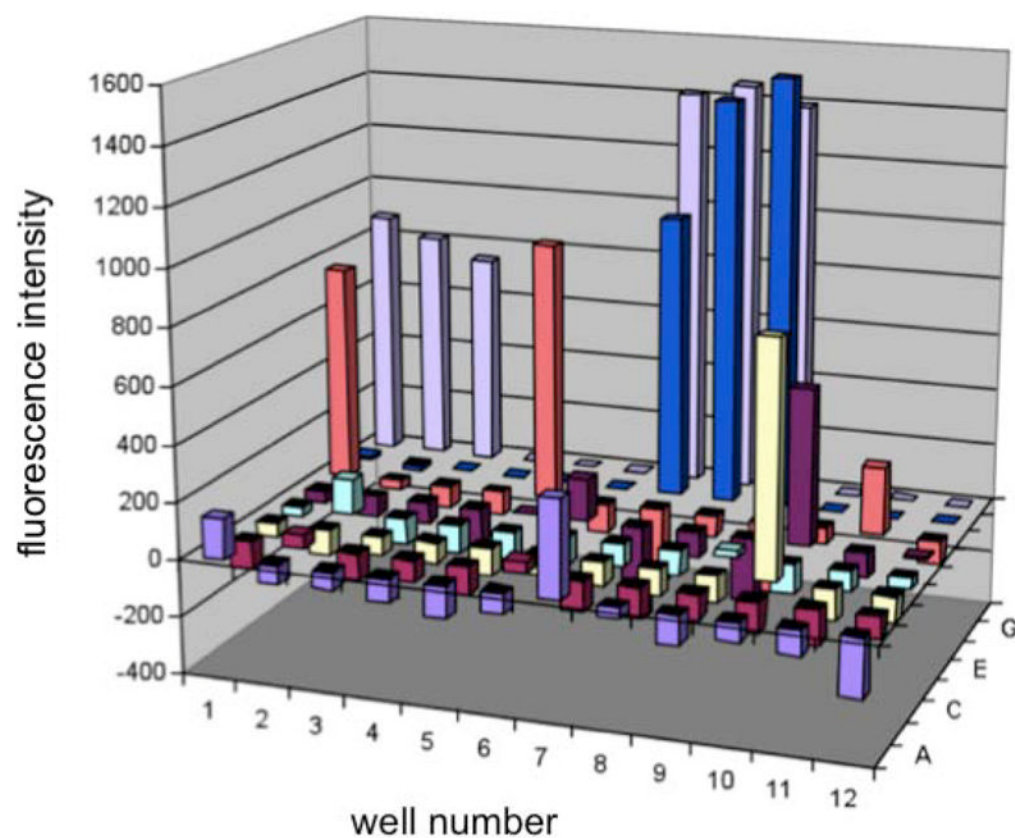
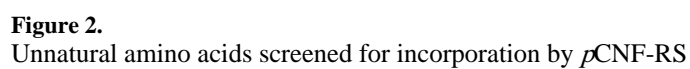


Figure 1.

GFP fluorescence assay for *p*CNF-RS dependent incorporation of unnatural amino acids into GFP_{Y151X}. A 96-well plate contains different non-native amino acids (1 mM, see supporting information) incubated with BL-21(DE3) cells harboring the GFP_{Y151X} reporter and the pEVOL-pCNF in 2YT media. Fluorescence was measured after 14 h at 30 °C of expression and corrected for background by a non-induced culture.



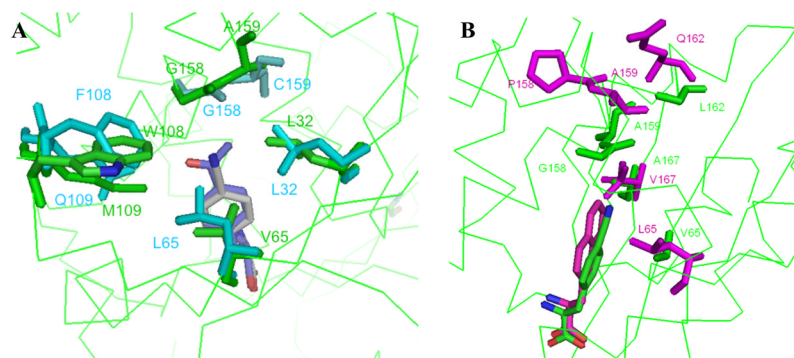


Figure 3.

A) Overlay of the key active site residues for substrate bound pAcF-RS·pAcF (cyan; PDB 1ZH6) and pCNF-RS·pCNF (green) complexes. The pAcF (blue) and pCNF (gray) substrates are shown at the center of the structure. B) Overlay of the substrate bound pNapA-RS·NapA (magenta, PDB 1ZH0) and pCNF-RS·pCNF (green) complexes. The NapA (magenta) and pCNF (green) substrates are shown at the bottom of the structure.

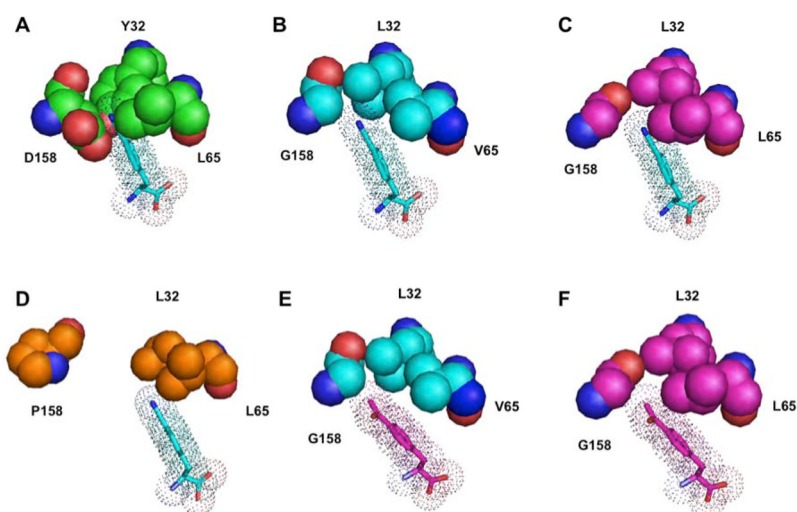


Figure 4. Structural analysis of 3 key residues (32, 65, and 158) for amino acid recognition in various synthetases. A) Wild-type tyrosyl RS (green, PDB 1J1U) modeled with *pCNF*. B) *pCNF*-RS (cyan) modeled with *pCNF*. C) *pAcF*-RS (magenta, PDB 1ZH6) modeled with *pCNF*. D) NapA-RS (orange, PDB 1ZH0) modeled with *pCNF*. E) *pCNF*-RS (cyan) modeled with *pAcF*. F) *pAcF*-RS (magenta, PDB 1ZH6) modeled with *pAcF*.

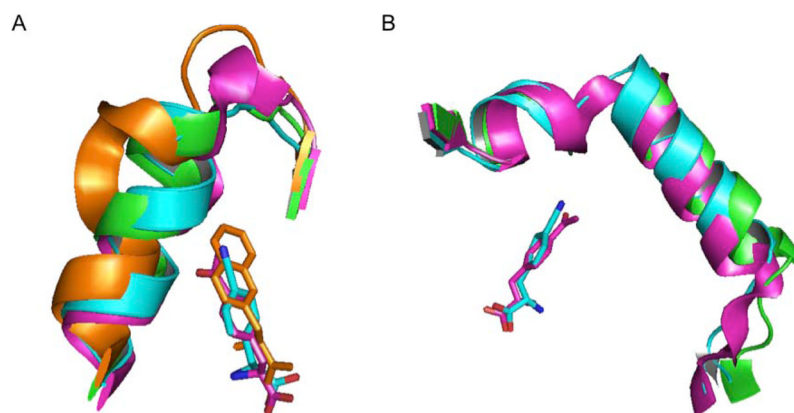


Figure 5.

Backbone perturbations in various aminoacyl-tRNA synthetases. A) Overlay of the helices containing mutated residues 158 and 159 in NapA-RS (orange; PDB 1ZH0), WT-TyrRS (green; PDB 1J1U), *pAcF*-RS (magenta; PDB 1ZH6) and *pCNF*-RS (cyan). The termination of the helix which accommodates large amino acids is especially apparent in NapA-RS B) Overlay of the helices containing mutated residues 108 and 109 in WT-TyrRS (green; PDB 1J1U), *pAcF*-RS (magenta; PDB 1ZH6) and *pCNF*-RS (cyan). *pCNF* = cyan, *pAcF* = magenta, NapA = orange.

Table 1

Data and refinement statistics

Space Group	P2 ₁
Unit Cell Å	a=52.52Å,b=68.93Å,c=82.09Å β=90.59
Wavelength Å	0.9778
Resolution Å(highest resolution shell)	2.3 (2.34–2.3)
R _{merge} % (highest resolution shell)	0.066 (0.25)
Unique Refs	46732
Completeness % (highest resolution shell)	96.2 (76.6)
I/sigma (Highest resolution shell)	15.0 (2.1)
Redundancy (highest resolution shell)	3.0(2.1)
Refinement	
R _{factor} (R _{free} [*]) % [†]	0.23 (0.30)
No. protein atoms	4913
No. water atoms	172
No. Hetero Atoms	28
rmsd bonds Å	0.013
rmsd angles °	1.37
Mean B factor Å ²	47.9

[†]R_{factor} = $\sum \sum |I_i - \langle I_i \rangle| / \sum |I_i|$ where I_i is the scaled intensity of the i th measurement, and $\langle I_i \rangle$ is the mean intensity for that reflection.

^{*}R_{free} = as for R_{cryst}, but for 5.0% of the total reflections chosen at random and omitted from refinement.

[§]Estimated overall coordinate error

Table 2

Unnatural amino acid incorporation by pCNF-RS.

aaRS	UAA	Expected ^[a]	Observed	Relative % Expression ^[b]
WT ^[c]	Phe ^[c]	18352	18353	100 ± 3.9
pCNF	1	18377	18376	79 ± 2.9
pCNF	2	18478	18477	87 ± 2.2
pCNF	3	18431	18431	96 ± 1.4
pCNF	4	18386	18386	91 ± 5.2
pCNF	5	18370	18368	45 ± 4.9
pCNF	6	18376	18376	84 ± 1.4
pCNF	7	18394	18396	60 ± 3.0
pCNF	8	18393	18393	95 ± 2.3
pCNF	9	18450	18450	43 ± 6.1
pCNF	10	18394	18393	82 ± 3.9
pCNF	11	18396	18395	75 ± 3.7
pCNF	12	18429	18326	81 ± 1.2
pCNF	13	18396	18394	61 ± 1.8
pCNF	14	18406	18405	72 ± 3.0
pCNF	15	18382	18382	45 ± 4.2
pCNF	16	18383	18383	94 ± 1.4
pCNF	17	18407	18407	77 ± 3.2
pCNF	18	18422	18422	61 ± 4.6

^[a]LC/MS expected mass for UAA incorporated into F107TAG myoglobin^[b]Based on GFP-Y151TAG expression, and normalized to WT GFP expression (16 mg/L)^[c]Mass for wild type Myo with Phe at residue.